

Unsteady rheometry: can we characterize weak gels with a controlled stress rheometer?

Christophe Baravian · Ghania Benbelkacem · François Caton

Received: 19 May 2006 / Accepted: 29 August 2006 / Published online: 15 November 2006
© Springer-Verlag 2006

Abstract This paper is concerned with the influence of apparatus inertia effects in controlled stress rheometry. As evidenced on creep experiments, the coexistence of apparatus inertia and viscoelasticity leads to a coupling frequency. For weak gels, this coupling frequency is typically between 1 and 100 Hz. Therefore, frequency sweeps around and above this coupling frequency also corresponds to an effective shear stress sweep evolution due to a non-trivial resonant effect. In other words, frequency sweep experiments are not made at constant shear stress. The detailed modelling and analysis of this inertia effect on a typical weak gel shows a clear and fundamental limitation for its characterization using a controlled stress rheometer. Also, alternative approaches to standard rheometer software analysis are proposed to take this coupling effect into account.

Keywords Unsteady rheometry · Weak gels · Control stress rheometer · Inertia effects

Introduction

Unsteady behaviour of complex fluids, like thixotropy and viscoelasticity is of fundamental importance in many industrial processes. While trying to measure these properties in a controlled stress rheometer, inertia effects have to be closely analysed to obtain the true material properties: Krieger (1990); Baravian and Quemada (1998a,b); Mackay et al. (1992); Frank (1992).

This paper was presented at the 3rd Annual Rheology Conference, AERC 2006, April 27-29, 2006, Crete, Greece.

C. Baravian (✉) · G. Benbelkacem · F. Caton
LEMTA CNRS UMR 7563 2, University of Nancy,
Avenue de la Forêt de Haye, BP,
160 54504 Vandoeuvre lès Nancy Cedex, France
e-mail: christophe.baravian@ensem.inpl-nancy.fr

In controlled-stress rheometers, apparatus inertia effects have been first studied by I. Krieger (1990) and can be expressed as the momentum equation of the mobile part of the rheometer:

$$I \frac{\partial^2 D}{\partial t^2} = \Gamma_{\text{applied}} - \Gamma_{\text{effective}} \quad (1)$$

where I is the inertia momentum of the mobile part, D the axis angular displacement and Γ_{applied} and $\Gamma_{\text{effective}}$, respectively, the applied and the effective torques felt by the material. For linear materials, Eq. 1 can be written as:

$$\alpha \frac{\partial^2 \gamma}{\partial t^2} = \sigma_{\text{applied}} - \sigma_{\text{effective}} \quad \text{with } \alpha = \frac{IF_{\sigma}}{F_{\gamma}} \quad (2)$$

where γ is the deformation, σ_{applied} and $\sigma_{\text{effective}}$ the shear stress applied by the rheometer and the effective shear stress felt by the material, respectively. α is the inertia parameter and involves the inertia momentum of the mobile part, but also the shear stress and shear rate geometry factors F_{σ} and F_{γ} of the geometry. Equation 2 simply expresses that the effective shear stress felt by the material is indeed different from the applied shear stress when inertia effects are involved. Inertia problems are also solved if the effective shear stress is properly evaluated.

As proposed by Krieger (1990), the effective torque in Eq. 1 can be evaluated by performing a first-order derivation of the measured angular velocity or a second-order derivation of the acquired angular displacement. This may be difficult, even on modern rheometers, as the accuracy depends on both angular precision and data acquisition rate. The obvious solution is a direct measurement of the torque transmitted to the sample, a solution

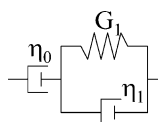
that is usually not implemented in controlled-stress rheometers, in contrast to rheometers with a separate torque transducer.

An improved estimation of the effective torque for ramp experiments (taking into account their real staircase shape) can be found in Baravian and Quemada (1998a).

For fluids, another unsteady effect can occur, associated with the development of the flow field in the studied sample. This is known as fluid inertia, which can be evaluated through a typical vorticity diffusion time as $t_{\text{diff}} \approx \rho e^2 / \eta$, where ρ is the fluid density, η its dynamic viscosity and e the typical geometry gap. The characteristic time corresponding to apparatus inertia effects can be estimated through Eq. 2, the effective stress being replaced by $\eta \dot{\gamma}$: $t_{\text{inertia}} \approx \alpha / \eta$ (Baravian and Quemada 1998a). The ratio of these two characteristic times is independent on the fluid viscosity: $t_{\text{inertia}} / t_{\text{diff}} \approx \alpha / (\rho e^2)$. For a typical fluid density of 1,000 kg/m³, in a standard geometry ($e < 1$ mm and $\alpha > 0.01$ Pa s²), the apparatus inertia effect clearly outlasts vorticity diffusion over at least one order of magnitude. Nevertheless, the effect of fluid inertia remains an instrumental limitation and can be accounted for in coaxial Couette geometry: Aschoff and Shümmer (1993); Hughes et al. (1998), and also in parallel plate geometry for oscillatory experiments: Böhme and Stenger (1990); Jones et al. (1987); Ding et al. (1999).

Instrumental inertia effects in controlled-rate rheometers also leads to a transitory regime, that cannot be modelled easily, as it is closely related to the feedback loop of the electronic device (Dullaert and Mewis 2005). As controlled-rate rheometers have a separate transducer to measure the torque, only the inertia of the transducer is relevant. Correction for transducer inertia is usually only necessary at high frequency.

The coupling between apparatus inertia and viscoelasticity stems for the inclusion in the inertia Eq. 2 of a material constitutive equation. For a Maxwell–Jeffreys model, the constitutive equation writes:



$$\eta_0 G_1 \dot{\gamma} + \eta_1 \eta_0 \ddot{\gamma} = (\eta_1 + \eta_0) \dot{\sigma} + G_1 \sigma \quad (3)$$

where the shear stress is the effective shear stress felt by the material. Therefore, by using Eqs. 2 and 3:

$$\underbrace{\alpha [(\eta_1 + \eta_0) \ddot{\gamma} + G_1 \ddot{\gamma}]}_{\text{Inertia}} + \eta_0 G_1 \dot{\gamma} + \eta_1 \eta_0 \ddot{\gamma} = (\eta_1 + \eta_0) \dot{\sigma}_{\text{applied}} + G_1 \sigma_{\text{applied}} \quad (4)$$

The form of Eq. 4 is very general. It is composed by an inertia term, involving not only the inertia parameter α but also viscoelastic constants and the general form of the

constitutive equation. Once the applied shear stress is defined for a given experiment, Eq. 4 can be solved, giving an analytical solution.

In this study, we analyse the coupling between apparatus inertia and viscoelastic properties of weak gels in controlled-stress oscillatory regime. In the first part, the existence of a coupling frequency is shown on a creep experiment. Then, we analyse raw data in the oscillatory regime and show that a resonant effect is nearly always present in standard rheometry. An analytical approach is used to understand this complex phenomenon on weak gels.

Creep experiment

When applying a shear stress step, inertia effects lead to “free” oscillations (Struik 1967; Roscoe 1969; Deiber and Peirotti 1995; Zölzer and Eicke 1993) when the elasticity is high enough (Baravian and Quemada 1998b). For a given model, these oscillations, due to inertia, can be used to characterize the material viscoelastic properties (Baravian and Quemada 1998b).

Solving Eq. 4 with $\sigma_{\text{applied}}(t) = \sigma_0 h(t)$, where σ_0 is the step stress amplitude and $h(t)$ the Heaviside function, we find:

$$J(t) = \frac{t}{\eta_0} - A + e^{-\lambda t} \left[A \cos(\omega t) + \frac{\lambda}{\omega} \left(A - \frac{1}{\lambda \eta_0} \right) \sin(\omega t) \right] \quad (5)$$

with $A = \frac{\alpha(\eta_1 + \eta_0)}{\eta_0 G_1} \left(\frac{2\lambda}{\eta_0} - \frac{1}{\alpha} \right)$, $\lambda = \frac{\alpha G_1 + \eta_1 \eta_0}{2\alpha(\eta_1 + \eta_0)}$ and $\omega = \sqrt{\frac{\eta_0 G_1}{\alpha(\eta_1 + \eta_0)} - \lambda^2}$ for $G_1 \geq \frac{2\eta_0^2}{\alpha} \left(1 + \frac{\eta_1}{2\eta_0} + \sqrt{1 + \frac{\eta_1}{\eta_0}} \right)$.

For times greater than the damping time $1/\lambda$, a standard retarded elasticity of the form $\sum_{i>1} \frac{1}{G_i} e^{-G_i t}$ can be used to model the compliance evolution with time, using the Boltzman superposition principle. The important result is that the frequency of oscillations H_c is well-defined as shown in Fig. 1. It can also be roughly estimated as $H_c = \frac{\omega}{2\pi} \cong \frac{1}{2\pi} \sqrt{\frac{G_1}{\alpha}}$, as generally $\eta_0 \gg \eta_1$ and $G_1/\alpha \gg \lambda$.

Figure 1 shows an experimental result on a creep experiment for a carbopol gel at 0.075% mass concentration (Carbopol 940 provided by BF Goodrich). A Maxwell–Jeffreys model is adjusted to the experimental data. The inertia parameter is $\alpha = 0.02$ Pa s² (AR2000, TA instrument and cone-plate geometry: 6 cm, 2°). We also show in Fig. 1 the same model response calculated for an ideal rheometer (without inertia). We can see that inertia can indeed be used to measure very accurately the viscoelastic properties of the studied sample (Baravian and Quemada 1998b). The oscillation frequency is, for this material, close to 8 Hz.

A simple mechanical analogy of the effect of inertia coupling for creep experiments is a mass attached to a spring that is dropped at the origin of time. When, instead

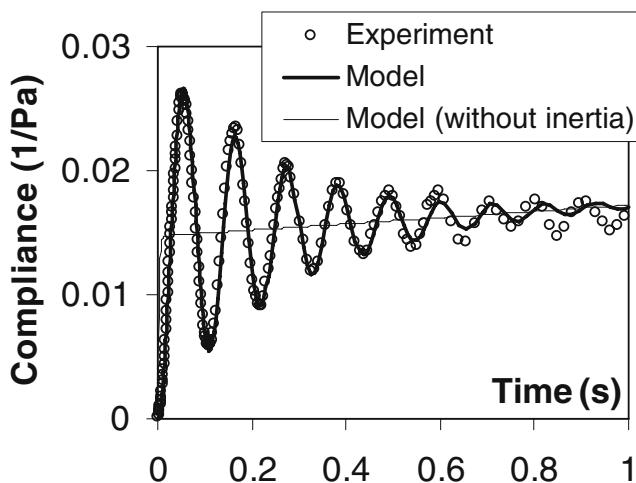


Fig. 1 Creep experiment for a 0.075% mass concentration of Carbopol 940. *Open circles* are experimental results. The *solid thick line* corresponds to adjustment of Eq. 5 with $G_1=68$ Pa, $\eta_1=0.16$ Pa s and $\eta_0=400$ Pa s. The *solid thin line* is the same Maxwell–Jeffreys model on an ideal rheometer without inertia

of a creep experiment, forced oscillations are performed on this mass-spring system, a resonant phenomenon is expected when the applied frequency H_0 is close to the coupling frequency H_c , leading to a divergence of the

deformation amplitude for an ideal linear spring. For weak gels, when deformation is increased, the material will react through a modification of its mechanical properties, leading to a nonlinear behaviour localized around the coupling frequency.

Forced oscillations

For forced oscillations, the applied shear stress is given by $\sigma_{\text{applied}}(t) = \sigma_0 \sin(2\pi H_0 t)$, where σ_0 is the amplitude of oscillations and H_0 the applied frequency. By replacing this expression in Eq. 4, we solve the motion equation for a Maxwell–Jeffreys model.

$$\gamma(t) = \frac{\sigma_0 \omega_0}{\alpha} \left\{ \frac{A_0}{\omega_0} \sin(\omega_0 t) - \frac{B_0}{\omega_0^2} \cos(\omega_0 t) - \frac{e^{-\lambda t}}{\lambda^2 + \omega^2} \times \left[C_0 \cos(\omega t) + D_0 \sin(\omega t) + \frac{B_0}{\omega_0^2} + \frac{C_0}{\lambda^2 + \omega^2} \right] \right\} \quad (6)$$

with $A_0 = \frac{\lambda^2 + \omega^2 - \omega_0^2 - 2\lambda G_1}{(\lambda^2 + \omega^2 - \omega_0^2)^2 + 4\lambda^2 \omega_0^2}$, $B_0 = \frac{G_1 - \eta_1 + 2\lambda \omega_0^2 A_0}{\eta_1 + \eta_0}$, $C_0 = -2\lambda A_0 - B_0$,

$D_0 = \frac{C_0 \lambda + A_0 (\lambda^2 + \omega^2)}{\omega}$ and $\omega_0 = 2\pi H_0$. Values of ω and λ are identical as defined for Eq. 5.

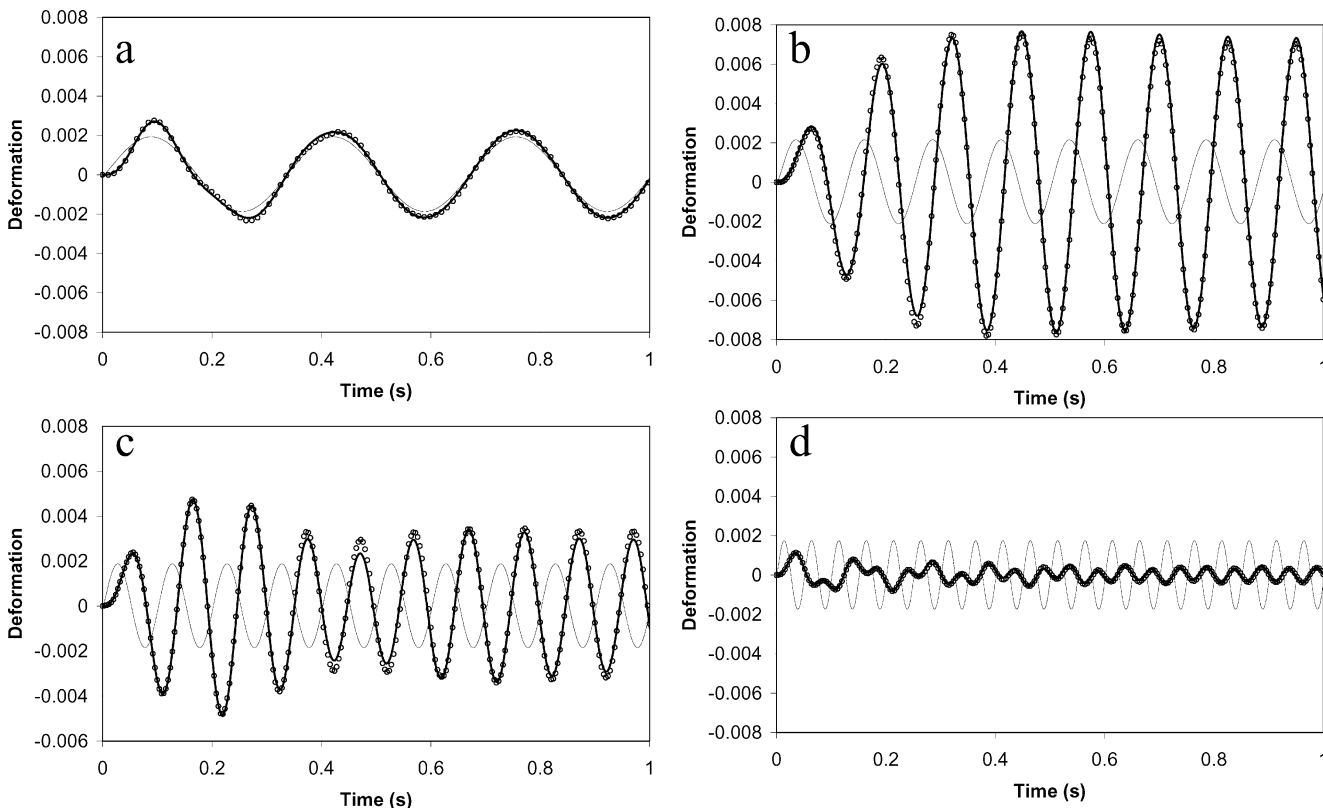


Fig. 2 Deformation vs time at various frequencies for an applied oscillation shear stress amplitude of 0.1 Pa. *Solid thick line*: adjustment of Eq. 6. *Solid thin line*: Same Maxwell–Jeffreys model on an ideal rheometer without inertia: **a** 3 Hz. $G_1=52.6$ Pa, $\eta_1=0.24$ Pa s and

$\eta_0=173$ Pa s; **b** 8 Hz. $G_1=45.8$ Pa, $\eta_1=0.21$ Pa s and $\eta_0=100$ Pa s; **c** 10 Hz. $G_1=53$ Pa, $\eta_1=0.14$ Pa s and $\eta_0=100$ Pa s and **d** 20 Hz. $G_1=56.6$ Pa, $\eta_1=0.07$ Pa s and $\eta_0=19.5$ Pa s

Figure 2 shows results at frequencies below, around and above the coupling frequency. On each experimental curve, the Maxwell–Jeffreys model is adjusted. To outline the importance of inertia effects for each experiment, the same model parameters are used to calculate the material response to an ideal rheometer (without inertia). We can see in Fig. 2 that below the coupling frequency (Fig. 2a), there is no real difference between the actual response and the ideal response once the transient behaviour ends. The characteristic time associated to this transient response depends on material viscoelasticity and rheometer inertia and is present in all experiments presented in Fig. 2. Its order of magnitude can be estimated for a Maxwell–Jeffreys model as $1/\lambda \approx 0.2$ s, which also corresponds to the characteristic time for the oscillation damping in the creep experiment (Fig. 1).

In the case of forced oscillations, the amplitude and frequency shifts are still very different from the ideal response even after this coupling time, unlike in creep experiments (Fig. 1), because the mechanical system is continuously forced. The amplitude of deformation increases strongly around the coupling frequency (Fig. 2b) and decreases above its value (Fig. 2d).

It is remarkable in Fig. 2 that the complex deformation responses can be very accurately modelled with a simple linear Maxwell–Jeffreys model. Actually, different model parameters are determined for each applied frequency and each applied shear stress amplitude by fitting the model over the first second.

From the model parameters adjusted on each experimental curve, we can calculate the effective shear stress from Eqs. 2 and 6. The asymptotic solution for the effective shear stress in oscillation experiments can be expressed as:

$$\sigma_{\text{effective}} = \sigma_0 A \sin(\omega_0 t + \delta) \tag{7}$$

with $A = \left[(1 + A_0 \omega_0^2)^2 + B_0^2 \omega_0^2 \right]^{1/2}$ and $\delta = \frac{B_0 \omega_0}{1 + A_0 \omega_0^2}$.

In Fig. 3, we represent the amplitude of the effective shear stress ($\sigma_0 A$) after the transient time (typically at 1 s). This effective shear stress is clearly different from the applied shear stress when the applied frequency H_0 is not small compared to the coupling frequency H_c and is also varying in time during the transient time. The resonant frequency is clearly seen around 8 Hz. Below this frequency, the effective shear stress increases, leading to a theoretical divergence at the coupling frequency. This divergence is in practice never attained, as the material reacts to this shear stress increase by a modification of its material properties through a reduction of its elasticity, which slightly (but sufficiently) shifts the coupling frequency (Fig. 3b).

Figure 4 shows deformation experiments for the same oscillation amplitude of 0.1 Pa, performed in superposition

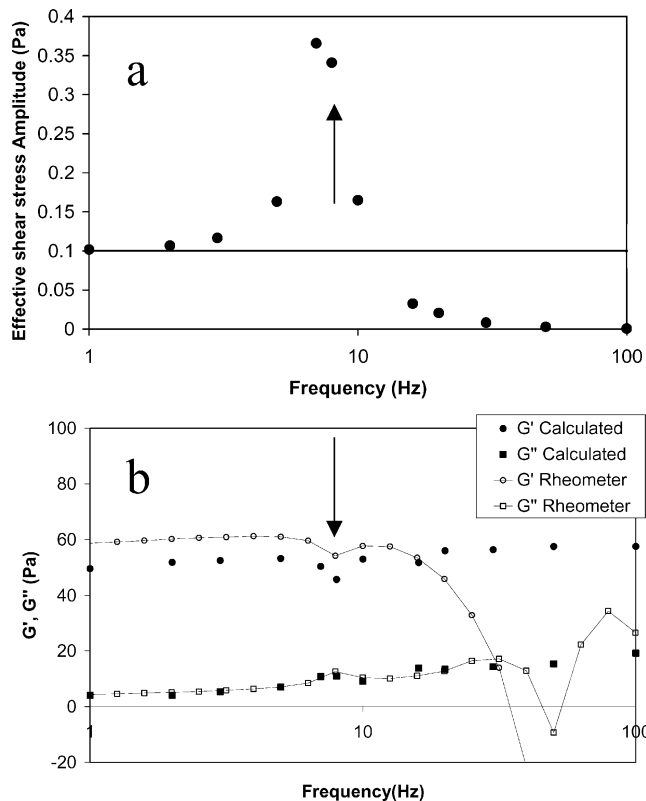


Fig. 3 **a** Effective shear stress amplitude in the steady state regime (Eq. 7). The *solid line* corresponds to the applied shear stress. **b** Comparison of shear modulus G' (circular symbols) and G'' (square symbols). Closed symbols: calculated from the model (Eq. 6) on deformation vs time data (Fig. 1). Open symbols: standard analysis from TA Instruments software

to a constant applied shear stress of 0.3 Pa. Close to the coupling frequency (around 8 Hz), the material reacts in a strongly nonlinear way as it starts to flow. In this case, the total effective shear stress amplitude is larger than the yield stress of the material (close to 0.7 Pa). When the applied frequency is larger than the coupling frequency, the

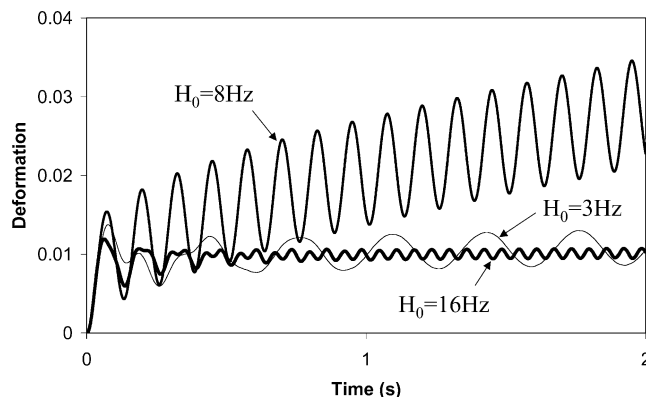


Fig. 4 Deformation experiments for an applied shear stress $\sigma_{\text{applied}}(t) = 0.3 + 0.1 \sin(2\pi H_0 t)$ with $H_0 = 3$ Hz, $H_0 = 8$ Hz and $H_0 = 16$ Hz. Close to the resonance ($H_0 = 8$ Hz), the material flows

effective shear stress amplitude is significantly smaller than the applied shear stress (Figs. 3a and 4) and even drops to zero (Fig. 3a). This clearly shows that frequency sweeps are not performed at constant effective shear stress.

Figure 3b also shows the results from the standard rheometer analysis of oscillations. These experiments have been performed independently using the standard oscillation data treatment of the rheometer software (oscillations over 6 s, with analysis of the last 3 s). Despite the internal correction of inertia present in the oscillation software analysis, the rheometer fails in giving correct values for G' and G'' above the coupling frequency, leading to negative G' values for frequencies greater than 30 Hz. From the model parameters adjusted on the direct deformation vs time response, G' and G'' values can be calculated as $G' = \frac{\omega_0^2/G_1}{1/\eta_0^2+(1+\eta_1/\eta_0)\omega_0^2/G_1^2}$ and $G'' = \omega_0 \frac{1/\eta_0+(1+\eta_1/\eta_0)\eta_1\omega_0^2/G_1^2}{1/\eta_0^2+(1+\eta_1/\eta_0)\omega_0^2/G_1^2}$. These values are compared to forced oscillations in Fig. 3b. The results are much more self-consistent, especially at frequencies higher than the coupling frequency.

Conclusion

This study shows that oscillation experiments for weak gels in controlled-stress rheometry have to be very carefully interpreted. Apparatus inertia and material elasticity lead to a coupling frequency that needs to be evaluated. For instance, its evaluation is accessible through a creep experiment or a G' measurement for a sufficiently low frequency experiment $H_0 \ll H_c \cong \frac{1}{2\pi} \sqrt{\frac{G'}{a}}$. For a standard geometry in controlled-stress rheometers, this coupling inertial effect will always be present between 1 and 100 Hz for sample elasticity smaller than 10,000 Pa. So, apparatus inertia effects are always present for weak gels.

For oscillation measurements, this coupling frequency is a fundamental limitation, because performing a frequency sweep around and above this coupling frequency will also correspond to a shear stress sweep (Fig. 3a): around the coupling frequency, the effective shear stress is much greater than the applied shear stress, and for frequencies above the coupling frequency, the effective shear stress is strongly decreased, dropping to zero at high frequency. The use of the simple analytical approach described in this paper can improve the accuracy of oscillatory analysis and

provides a very accurate description of the viscoelastic behaviour of the material in creep experiments.

To overcome this fundamental limitation in controlled-stress rheometers (also present when these rheometers are used in the controlled strain mode), specially designed transducers have to be developed for an active control of the effective shear stress.

Acknowledgments We thank Bernard Costello from TA Instruments for providing the program software that allowed direct control of the motor and raw results from the displacement encoder. All displacement experiments (Figs. 2 and 4) were obtained with this specially designed software.

References

- Aschoff D, Shümmer P (1993) Evaluation of unsteady Couette-flow measurement under the influence of fluid inertia. *J Rheol* 37(6):1237–1251
- Baravian C, Quemada D (1998a) Correction of instrumental inertia effects in controlled stress rheometry. *Eur Phys J Appl Phys* 2:189–195
- Baravian C, Quemada D (1998b) Using instrumental inertia effects in controlled stress rheometers. *Rheol Acta* 37:223–233
- Böhme G, Stenger M (1990) On the influence of fluid inertia in oscillatory rheometry. *J Rheol* 34(3):415–424
- Deiber JA, Peirotti MB (1995) Free damped oscillations of the linear viscoelastic material. *Rheol Acta* 34:317–320
- Ding F, Giacomin AJ, Bird RB, Kweon C-B (1999) Viscous dissipation with fluid inertia in oscillatory shear flow. *J Non-Newtonian Fluid Mech* 86:359–374
- Dullaert K, Mewis J (2005) Thixotropy: build-up and breakdown curves during flow. *J Rheol* 49(6):1213–1230
- Frank AJP (1992) Importance of inertia for controlled stress rheometers. In: *Theoretical and Applied Rheology*. Elsevier Science, Belgium
- Hughes JP, Davies JM, Jones TER (1998) Concentric cylinder end effects and fluid inertia effects in controlled stress rheometry I. Numerical simulation. *J Non-Newton Fluid Mech* 77:79–101
- Jones TER, Davies JM, Thomas A (1987) Fluid inertia effects on a controlled stress rheometer in its oscillatory mode. *Rheol Acta* 26:14–19
- Krieger I (1990) The role of instrument inertia in controlled-stress rheometers. *J Rheol* 34:471–483
- Mackay ME, Liang C-H, Halley PJ (1992) Instrument effects on stress jump measurements. *Rheol Acta* 31:481–489
- Struik LCE (1967) Free damped vibrations of linear viscoelastic materials. *Rheol Acta* 6:119–129
- Roscoe R (1969) Free damped oscillations in viscoelastic materials. *J Phys D Appl Phys* 2(2):1261–1266
- Zölzer U, Eicke H-F (1993) Free oscillatory shear measurements—an interesting application of constant stress rheometers in the creep mode. *Rheol Acta* 32:104–107